Disentanglement of the electronic properties of metallicity-selected single-walled carbon nanotubes

P. Ayala,[1] Y. Miyata,[2,3] K. De Blauwe,[1] H. Shiozawa,[4] Y. Feng,[5] K. Yanagi,[5] C. Kramberger,[1] S. R. P. Silva,[4] R. Follath,[6] H. Kataura,[5,7] and T. Pichler[1]

[1]*Faculty of Physics, University of Vienna, 1090 Wien, Austria*

[2]*Nanotechnology Research Institute, National Institute of Advanced Industrial Science and Technology, Tsukuba 305-8562, Japan*

[3]*Department of Chemistry, Nagoya University, Nagoya 464-8602, Japan*

[4]*Advanced Technology Institute, University of Surrey, Guildford GU2 7XH, United Kingdom*

[5]*Nanotechnology Research Institute, National Institute of Advanced Industrial Science and Technology, Tsukuba 305-8562, Japan*

[6]*BESSY II, D-12489 Berlin, Germany*

[7]*JST, CREST, Kawaguchi, Saitama 330–0012, Japan*

(Received 26 October 2009; published 30 November 2009)

The inherent structure of single-walled carbon nanotubes (SWCNTs) provides them tremendous value as archetypical one-dimensional (1D) solids, which exhibit van Hove singularities in their local density of states, Tomonaga-Luttinger liquid behavior, ballistic transport properties, and in many other aspects, features of 1D quantum systems, which allow the study of fundamental problems. Therefore, unraveling the signature of their peculiar electronic structure as pristine material is a prerequisite for tracing any modification. Here, we show the disentanglement of the unique 1D features and bonding environments in clean metallicity sorted nanotube films. The photoemission and x-ray absorption responses unambiguously reveal how the fine structure in the C1s edge and photoemission valence band separately discerns the SWCNT metallic and semiconducting nature. This has crucial implications for applications allowing for instance finding the limit of maximum conductivity in transparent electrodes or the uniformity of power transistors, among others.

DOI: 10.1103/PhysRevB.80.205427 PACS number(s): 71.20.Tx, 71.10.Hf, 73.63.Fg

I. INTRODUCTION

Single-walled carbon nanotubes (SWCNTs) have turned into a technological and scientific spotlight, propelled to an unprecedented level after Iijima´s reported observations in transmission electron microscopy (TEM).[1] The mechanical and electronic properties of these structures are mainly given by their internal arrangement of C atoms with sp^2 hybridization. This geometrical organization gives raise to metallic or semiconducting SWCNTs with exceptional features. They are ideal one-dimensional (1D) conductors with unusual transport properties such as ballistic transport and Tomonaga-Luttinger liquid (TLL) ground state (in metallic tubes).[2] SWCNTs exhibit in many other aspects properties of 1D quantum systems, in which fundamental problems can be studied. This makes them one of the most promising materials to study tunable correlation effects. However, one of the imminent problems toward applications has been the production of mixtures of semiconducting and metallic species. Still, experiments with different methods, using bulk samples of SWCNT (mats) with mixed metallicity, have made possible the identification of their corresponding van Hove singularities (vHs). These features, which are characteristic of the 1D density of states (DOS) of the SWCNTs, are visible in the differential conductance,[3] the loss-function,[4] the optical absorption (OAS),[5] photoemission (PES),[6,7] and C1s x-ray absorption (XAS) response.[8] It has also been feasible to confirm the 1D Tomonaga-Luttinger power law scaling by valence band PES[6,7] and nuclear magnetic resonance (NMR).[9] In this context, the recent advances toward sorting out SWCNTs according to metallicity have opened the possibility to study experimentally long theoretically predicted phenomena. Nowadays, it is possible to perform separation of nanotubes with electrophoresis-based as well as ultracentrifugation-based techniques. For the material shown here, we have used nanotubes separated via density gradient ultracentrifugation (DGU), which is one of the most efficient and clear ways to attain metallicity sorting.[10]

In this work, we have used metallicity sorted samples, which additionally exhibit a very narrow Gaussian diameter distribution centered at 1.37 nm. The very small spread of 0.08 nm ensures the availability of SWCNTs in a range of uniform energy gap distribution, which enables us to access the bulk electronic properties of metallicity selected mats of SWCNTs. These properties are here unraveled with a combined high resolution PES and XAS approach. As a result, the TLL power law scaling in bulk metallic SWCNTs in the metallic ground state is presented together with a core level PES study, which reveals a textbook example for metallic and semiconducting sp^2 carbon systems owing a narrow C1s response. The metallic tubes exhibit an asymmetric Doniac-Sunijic form, while the semiconducting C1s display a symmetric Voigtian. Using valence band PES and XAS we show the individual manifestation of the 1D band structure and directly probe all vHs in the occupied and unoccupied DOS, respectively. The observed vHs are in very good agreement with diameter cumulative tight binding (TB) predictions after accounting for different work functions in semiconducting and metallic tubes. These results are a direct assessment of the 1D electronic structure of SWCNTs and provide a solid basis to analyze the influence of doping and chemical interactions on their electronic transport properties.

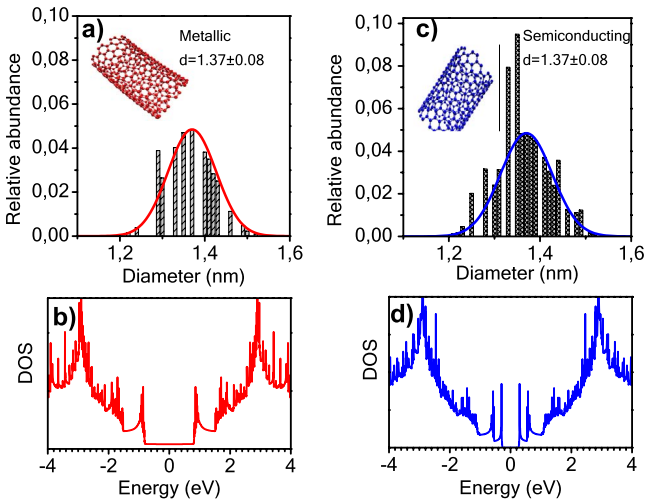

FIG. 1. (Color online) Schematics showing the relative abundance of metallicity sorted nanotubes and the corresponding fraction of the DOS. The histograms illustrate the abundance of metallic (left) and semiconducting (right) SWCNTs within the diameter range given from Raman spectroscopy and optical absorption measurements. The diameter distribution is a Gaussian centered at 1.37 nm and it has a 0.8 nm spread. The lower figures show the respective fraction of the TB DOS of the semiconducting and metallic SWCNTs.

II. EXPERIMENTAL

Films of purified SWCNTs with a characteristic narrow Gaussian diameter distribution centered at 1.37 nm and a spread of 0.08 nm have been probed here. The SWCNTs were produced by arc discharge and DGU was used to achieve metallicity separation.[11] A subsequent filtration was used to form mats of metallic and semiconducting SWCNTs. The mats were then transferred onto sapphire plates, mounted onto a copper sample holder and annealed at 1000 K in a UHV preparation chamber. The PES and XAS experiments were performed at beamline UE 52 PGM at BESSY II, which has a resolving power $(E/\Delta E)$ of 4×10^4.[12] For PES, a hemispherical photoelectron energy analyzer SCIENTA SES 4000, with the energy resolution set to 10 meV, was used. XAS was conducted with the total electron yield mode at 15 K with an effective energy resolution better than 30 meV. The excitation energies were calibrated by the Fermi edge of clean Au films and the XAS response was normalized to their background absorbance. In all cases, the sample stoichiometry and purity were checked by a PES survey scan up to 1200 eV (as the inset in Fig. 1). No contamination from oxygen or catalyst particles was detected in any sample within the experimental limit of 0.5%. For the diameter cumulative first order TB calculations[8,13] we used an overlap integral of $\Gamma_0=2.95$ eV and the above mentioned Gaussian diameter distribution of 1.37 ± 0.08 (see Fig. 1).

III. RESULTS AND DISCUSSION

The C1s core level response in PES and XAS is widely studied feature for various carbon systems. These responses are indeed very useful because their shape is related to the final state effects of the conduction electrons. As a prerequisite for all our measurements, the sample stoichiometry and purity were checked by a PES survey scan up to 1200 eV in all cases as mentioned in the experimental section. No contamination from oxygen or catalyst particles was detected in any sample within the experimental limit of 0.5%. The C1s responses and nanotube particular features are here nicely unraveled examining samples that have measured up the long-expected availability of metallicity selected SWCNTs. Figure 2 displays the C1s response in PES with unprecedented detail. The C1s lines of the metallicity separated SWCNTs obtained by high resolution PES, using a 400 eV photon energy, are depicted.

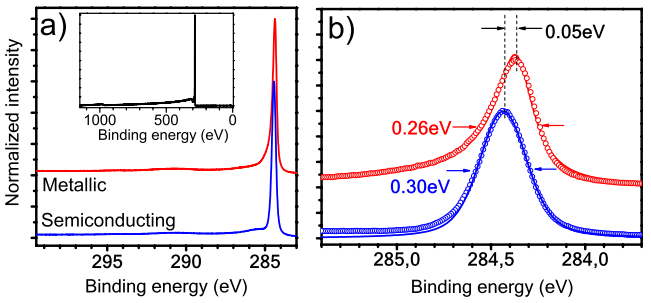

FIG. 2. (Color online) (a) C1s photoemission of metallic SWCNT (upper curve) and semiconducting SWCNT (lower curve) as conducted at 400 eV photon energy. The inset shows a PES survey scan up to 1200 eV. (b) The C1s line of the metallic and semiconducting SWCNT on an expanded scale. The solid lines are fits using a line shape analysis with a Doniach-Sunjic (metal) and Voigtian line shapes (semiconductors).

Evaluating the narrow shape of the C1s PES line on Fig. 2(b), peak maxima at binding energies of 284.48 and 284.43 eV are clearly observed, for the metallic and semiconducting SWCNTs, respectively. A one to two superposition of the metallic and semiconducting SWCNTs response clearly resolves earlier hypotheses for mixed metallicity SWCNTs.[8,14,15] As observed in Fig. 2(b), there is a 0.05 eV downshift in the binding energy for the metallic SWCNTs, which can be related to two effects. First, the possibility of different core hole screening in metallicity selected SWCNTs,[16] and then, the possibly different chemical potentials in bulk metallicity selected SWCNTs.[17] As discussed later, core hole effects are not visibly affected by metallicity, which leads us to suggest that the different core level binding energy in metallicity selected SWCNTs is mainly due to differences in the chemical potentials. The line shape analysis in Fig. 2(b) reveals an asymmetric Doniach-Sunjic line profile[18] convoluted with a Gaussian for the metallic SWCNTs. We find an asymmetry parameter $\alpha=0.11$, which is in good agreement with previous studies on graphite.[19] The full width at half maximum (FWHM) of the C1s peak of the metallic SWCNTs is 0.26 eV, which is surprisingly slightly narrower than the 0.32 eV of graphite.[20] This could be attributed to the different metallicity and coupling strength in the metallic SWCNTs and in graphite. In contrast, a symmetric C1s line with a Voigtian lineshape is observed in the semiconducting SWCNTs. The line shape analysis reveals a FWHM of 0.30 eV, which is comparable to graphite

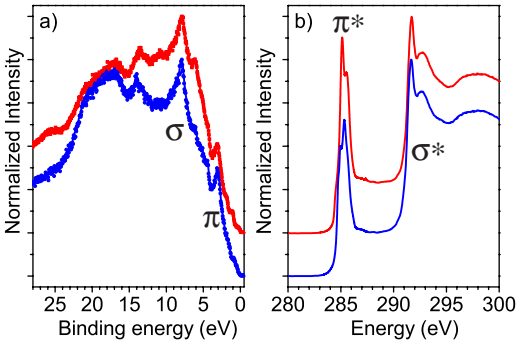

FIG. 3. (Color online) (a) Valence band photoemission spectra of metallic (upper curve) and semiconducting (lower curve) conducted at 150 eV photon energy. (b) High-resolution XAS response of metallic (upper curve) and semiconducting (lower blue curve).

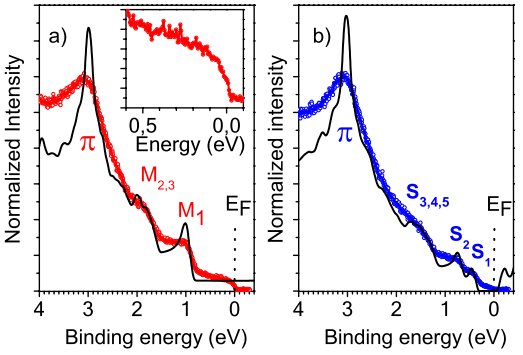

FIG. 4. (Color online) π band response in the valence band PES conducted at 150 eV for the metallic (a) and the semiconducting SWCNTs (b). The inset in a shows the expanded region around E_F on an expanded scale. The black lines in the main panels show the fraction of the TB DOS of the semiconducting and metallic SWCNTs probed. The diameter cumulative TB DOS in Figs. 1(b) and 1(d) are broadened by the experimental resolution and the labels $M_{1\cdots3}$ and $S_{1\cdots5}$ depict the position of the vHs.

but lower than, for instance, the 0.35 eV in C_{60}.[21] The increased linewidth in C_{60} stems from the molecular band structure and curvature, yielding slightly different environments for the individual carbon atoms. Still, for neither type of metallicity selected SWCNTs an increased broadening in comparison to graphite is evidenced. The C1s linewidth in SWCNTs is apparently directly related to the planar graphene lattice and it can be taken as a text-book example of the intrinsic C1s response of semiconducting 1D sp^2 carbon systems. Whatever the case may be, the Gaussian spread of SWCNTs diameters is also not reflected in the SWCNTs C1s line width.

It is well known that high-resolution valence band PES and XAS are versatile tools to probe the matrix element weighted density of occupied and unoccupied states, respectively. In the PES case, we have analyzed on the whole valence band of the metallicity selected SWCNTs employing an excitation energy of 150 eV (see Fig. 3). As expected from the C1s response, the overall features of electronic π and σ states at binding energies above 2.5 eV are reminiscent of the band structure of graphene. It is also worth noting a higher spectral weight of the lower shoulder of the σ peak at 6.2 eV binding energy for the metallic SWCNTs.

In the case of the XAS response, the signature of the conduction band in the metallicity separated SWCNTs is also provided in Fig. 3. The overall shape is again reminiscent for graphite with the well known $\pi^\star$ resonance at 285.4 eV and the $\sigma^\star$ threshold at 291.7 eV,[22] which is also in good agreement with core level EELS of the C1s edge of SWCNTs[23] and with XAS results on SWCNTs.[14,15,24] However, a second key feature appears in the XAS C1s response of these separated nanotubes. This is a clear fine structure in the $\pi^\star$ resonance, which can be related to the distinct vHs in the unoccupied DOS of the SWCNTs.[8] The XAS spectra show clearly resolved fine structure features, which selectively address the concomitant response of metallicity sorted SWCNTs. This discerns unambiguously the fine structure that fingerprints the 1D response of metallic and semiconducting SWCNTs.

To deepen into the analysis of this fine structure, we show a detailed close up of the valence band response at low-binding energies of the metallic SWCNTs in Fig. 4(a) and that of semiconducting SWCNTs in Fig. 4(b). Both the π band response at a binding energy of 3 eV, which is related to the high DOS at the M point in graphene, as well as the respective diameter cumulative vHs of the metallic and semiconducting SWCNTs are observed. The S_1 and S_2 peaks at 0.44 and 0.75 eV are only observed in the semiconducting SWCNTs, whereas the M_1 peak at 1.05 eV is only observed in the metallic SWCNTs. In addition to these peaks, we report here the first observation of the higher order vHs of the cumulative DOS. Because of their overlapping, these vHs are not perfectly separated and therefore we have only indicated them as $M_{2,3}$ at 1.8 and 2 eV and as $S_{3,4,5}$ at 1.32, 1.5, and 1.72 eV, correspondingly. The overlapping higher vHs peaks are reminiscent of a uniform distribution in chiral angles in the specimen. Bearing in mind the results of the diameter cumulative first-order TB calculations, which are also depicted for the metallic SWCNTs and semiconducting SWCNTs in Figs. 1(b) and 1(d), the positions and the overall shape of the vHs simulated and broadened with the experimental resolution [solid black lines in Figs. 4(a) and 4(b)] are perfectly associated with the recorded signals for both the metallic and the semiconducting SWCNTs. In order to compare the experiments in the main panels in Fig. 4, a 30 meV resolution broadening was applied to the spiky diameter cumulative DOS. The direct comparison reveals an additional energy dependent broadening in the PES spectra, and that is attributed to the decreasing lifetime of the excited state. The comparison to the TB calculations is better if the Fermi level (E_F of metallic SWCNTs is symmetric regarding the occupied and unoccupied DOS. On the other hand, for the semiconducting SWCNTs a charge neutrality level about 0.1 eV above the center of the gap fits best to our calculations, i.e., 0.1 eV toward the conduction band. This strongly suggests a different chemical potential in the semiconducting SWCNTs in agreement with the above mentioned differences in the C1s binding energy.

Regarding the onset of the PES response at low-binding energies in the metallic tubes pinpointed in the lower left inset in Fig. 4(a), we observe the power law dependence of the photoemission response proportional to E^α of a TLL with α=0.37. This is slightly lower than the α=0.42–0.48 previ-

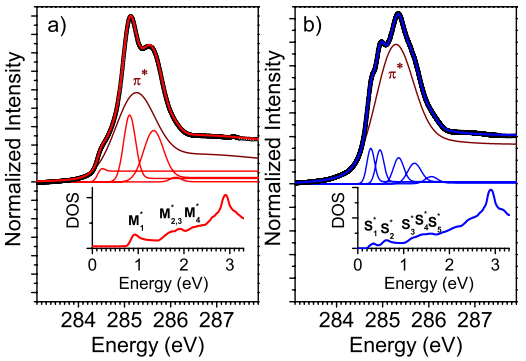

FIG. 5. (Color online) Close up of the high-resolution XAS C1s $\pi^\star$ absorbtion edges (circles) of metallic (a) and semiconducting SWCNT (b) together with the results of a line shape analysis (lines). The lower insets depict the diameter cumulative TB DOS broadened by the experimental resolution. The labels denote the vHs ($M^\star_{1\ldots4}$,$S^\star_{1\ldots5}$), and the overall conduction band ($\pi^\star$).

ously reported for SWCNT bundles with mixed metallicity.[6,7] At first glance this observation is quite surprising, since n-type intercalation of metallicity mixed bundles of SWCNTs reveals a transition from a TLL to a normal Fermi liquid as soon as all SWCNTs in a bundle are driven metallic.[7] However, in the present case the bulk metallicity in the all-metallic SWCNT bundles is still a 1D metallic phase. Apparently, there are insufficient interactions to break down the isolation of the 1D channels in the individual metallic SWCNTs within the bundles. This can be directly associated to the doping effect due to intercallation in bundles of SWCNTs. A recent report has proved that the transition to a three-dimensional Fermi level occurs only at doping levels which are high enough to occupy the first vHs of the former conduction band.[25] Our observation substantially reinforces this hypothesis suggesting that the interaction between different metallic tubes within a bundle of only metallic tubes is still small enough to stabilize a 1D TLL ground state. This has important implications on the maximum conductivity of mats of only metallic SWCNTs, for instance in their application as transparent conducting electrodes.

Contemplating now the 1D DOS in the conduction band of metallicity selected SWCNTs in high-resolution XAS at the C1s edge (see Fig. 5), the $\pi^\star$ response of the metallic (c) and semiconducting (d) SWCNTs exhibit a unique fine structure. To unravel the fine structures individually, we performed a line shape analysis using Gaussian components, which are illustrated by the solid lines (red metallic and blue semiconducting) for the response of the vHs and a broad Voigtian for the $\pi^\star$ peak (green solid line). The $\pi^\star$ peak is observed at 285.26 and at 285.3 eV for the metallic and semiconducting SWCNTs, which is in very good agreement to the values of graphite. For the metallic SWCNTs the additional foot at the low-binding energy was fitted using a cumulative Gaussian folded by a Fermi function. As can be seen by the thick red and blue solid lines in Figs. 5(a) and 5(b), we resemble our experimental data very closely in the full line shape analysis. The metallic fine structures are positioned at 285.10 eV, 285.65 eV and a shoulder at 286.1 eV. The semiconducting fine structures are observed as peaks at 284.75, 284.95, and 285.35 eV, and as shoulders at 285.7 and 286.05 eV. The additional foot in metallic SWCNTs is located at 284.5 eV. The comparison of the detailed line shape analysis to the broadened metallicity selected diameter cumulative DOS is shown in the lower insets in Figs. 5(a) and 5(b). The insets have been positioned according to the C1s binding energy which clearly resemble the respective XAS onsets. It is worth noting that in analogy to PES, the same fine structures ($S^\star_1$ to $S^\star_5$ and $M^\star_1$ to $M^\star_4$) are observed in high resolution XAS. For the metallic tubes the additional foot can be attributed the onset of the constant 1D DOS at the E_F. The actual positions and widths of the diameter cumulative vHs peaks are in very good agreement with the TB calculations without any further scaling, while the broad $\pi^\star$ resonance is known to be strongly affected by the C1s core hole. Previous studies on SWCNTs samples with mixed metallicity, reported a $\pi^\star$ peak related to the DOS at the M point of the underlying graphene structure downshifted by about 2 eV due to the C1s core hole effects,[8,26,27] i.e., it is strongly excitonic. On the other hand, in molecules like C_{60} (Ref. 21) and $C_{59}N$ (Ref. 28) the bands are associated to the molecular orbitals and the core hole effects are much less pronounced. Although the $\pi^\star$ peak is strongly excitonic and downshifted by core hole effects, our TB calculations allow directly identifying the individual fine structures in the unoccupied DOS in a straightforward manner. We find a clear twofold response: The core hole effect in the broad C1s $\pi^\star$ resonance just resembles bulk sp^2 carbon, and the diminutive core hole effects in the resonances due to vHs are typical for molecular excitations. The observed analogies hint on an intriguing composition of bulk and molecular features in the electronic excitation spectrum of SWCNTs. This also highlights some of the complications in correctly describing the details of the C1s response of this 1D solids in theory so far. Calculations such as the ones performed by Wessely *et al.*[29] yield correct signs and magnitudes of core hole effects when they are applied to selected chiralities with small unit cells. In contrast to TB, these calculations cannot be applied to the whole set of chiralities. One of the major gains of this XAS result is that it completes our knowledge on the 1D electronic structure of SWCNTs on the bulk scale by directly accessing the details in the conduction band. This represents a model or base to compare molecular-like conduction band DOS of the vHs in polarization perpendicular to the tube axis, such as in the well studied case of other molecular systems like functionalized fullerenes.[28]

IV. CONCLUSIONS

In summary, this combined high-resolution PES and XAS study on mats of metallicity selected SWCNTs sets the basis for understanding the intrinsic electronic properties of SWCNTs in unprecedented detail. This includes a textbook example of the intrinsic response of metallic and semiconducting 1D sp^2 hybridized graphitic systems, which also forges a pattern to further analyze the influence of doping and chemical interactions. The experimental electronic structure of the valence band (PES) and conduction band (XAS) reveals a very good agreement in the position of the vHs

determined by diameter cumulative TB calculations. Deviations are related to the different work functions in metallic and semiconducting SWCNTs as well as to strong core hole effects for the bulk XAS response. For the metallic SWCNTs we observe a TLL power low renormalization close to E_F. This study also pioneers the understanding of the electronic properties in 1D solids on the bulk scale and sets the basis for the future understanding of the complex interplay between charge transfer and hybridization in functionalized SWCNTs as perfectly 1D molecular solids. The fundamental understanding of these processes paves the way toward chemically functionalized and metallicity selected SWCNTs, which are in turn, a key ingredient in accessing the application potential of doped 1D hybrid systems for applications in nanoelectronics, nanooptics and nanochemistry.

ACKNOWLEDGMENTS

This work was supported by Projects No. P21333-N20 (from the FWF) and No. PI 440-4/5 (from the DFG). H.S. and S.R.P.S. acknowledge the Leverhulme Trust and the EPSRC through a Portfolio Partnership grant. We acknowledge the technical assistance from S. Leger, R. Hübel, and R. Schönfelder from the IFW-Dresden.

[1] S. Iijima, Nature (London) **354**, 56 (1991).
[2] S. Tomonaga, Prog. Theor. Phys. **5**, 544 (1950).
[3] T. W. Odom, J. L. Huang, P. Kim, and C. M. Lieber, Nature (London) **391**, 62 (1998).
[4] T. Pichler, M. Knupfer, M. S. Golden, J. Fink, A. Rinzler, and R. E. Smalley, Phys. Rev. Lett. **80**, 4729 (1998).
[5] H. Kataura, Y. Kumazawa, Y. Maniwa, I. Umezu, S. Suzuki, Y. Ohtsuka, and Y. Achiba, Synth. Met. **103**, 2555 (1999).
[6] H. Ishii *et al.*, Nature (London) **426**, 540 (2003).
[7] H. Rauf, T. Pichler, M. Knupfer, J. Fink, and H. Kataura, Phys. Rev. Lett. **93**, 096805 (2004).
[8] C. Kramberger, H. Rauf, H. Shiozawa, M. Knupfer, B. Buchner, T. Pichler, D. Batchelor, and H. Kataura, Phys. Rev. B **75**, 235437 (2007).
[9] B. Dora, M. Gulacsi, F. Simon, and H. Kuzmany, Phys. Rev. Lett. **99**, 166402 (2007).
[10] M. S. Arnold, A. A. Green, J. F. Hulvat, S. I. Stupp, and M. C. Hersam, Nat. Nanotechnol. **1**, 60 (2006).
[11] Y. Miyata, K. Yanagi, Y. Maniwa, and H. Kataura, J. Phys. Chem. C **112**, 13187 (2008).
[12] A. Scholl, Y. Zou, T. Schmidt, R. Fink, and E. Umbach, J. Electron Spectrosc. Relat. Phenom. **129**, 1 (2003).
[13] H. Shiozawa *et al.*, Phys. Rev. B **73**, 075406 (2006).
[14] A. Nikitin, H. Ogasawara, D. Mann, R. Denecke, Z. Zhang, H. Dai, K. Cho, and A. Nilsson, Phys. Rev. Lett. **95**, 225507 (2005).
[15] R. Larciprete, A. Goldoni, S. Lizzit, and L. Petaccia, Appl. Surf. Sci. **248**, 8 (2005).
[16] H. Shiozawa, T. Pichler, C. Kramberger, M. Rummeli, D. Batchelor, Z. Liu, K. Suenaga, H. Kataura, and S. R. P. Silva, Phys. Rev. Lett. **102**, 046804 (2009).
[17] W. S. Su, T. C. Leung, and C. T. Chan, Phys. Rev. B **76**, 235413 (2007).
[18] S. Doniach and M. Sunjic, J. Phys. C **3**, 285 (1970).
[19] K. C. Prince, I. Ulrych, M. Peloi, B. Ressel, V. Chab, C. Crotti, and C. Comicioli, Phys. Rev. B **62**, 6866 (2000).
[20] S. Suzuki, C. Bower, T. Kiyokura, K. G. Nath, Y. Watanabe, and O. Zhou, J. Electron Spectrosc. Relat. Phenom. **114**, 225 (2001).
[21] A. Goldoni, C. Cepek, R. Larciprete, L. Sangaletti, S. Pagliara, G. Paolucci, and M. Sancrotti, Phys. Rev. Lett. **88**, 196102 (2002).
[22] E. J. Mele and J. J. Ritsko, Phys. Rev. Lett. **43**, 68 (1979).
[23] T. Pichler, New Diamond Front. Carbon Technol. **11**, 375 (2001).
[24] A. Goldoni, R. Larciprete, L. Petaccia, and S. Lizzit, J. Am. Chem. Soc. **125**, 11329 (2003).
[25] C. Kramberger, H. Rauf, M. Knupfer, H. Shiozawa, D. Batchelor, A. Rubio, H. Kataura, and T. Pichler, Phys. Rev. B **79**, 195442 (2009).
[26] E. L. Shirley, Phys. Rev. Lett. **80**, 794 (1998).
[27] P. A. Bruhwiler, P. Kuiper, O. Eriksson, R. Ahuja, and S. Svensson, Phys. Rev. Lett. **76**, 1761 (1996).
[28] T. Pichler *et al.*, Phys. Rev. Lett. **78**, 4249 (1997).
[29] O. Wessely, O. Eriksson, and M. I. Katsnelson, Phys. Rev. B **73**, 075402 (2006).